Numerical Technique Based on Extended Boundary Node Method for Solving Grad-Shafranov Equation

Ayumu Saitoh[1], Taku Itoh[2], Nobuyuki Matsui[3], and Atsushi Kamitani[4]

[1]University of Hyogo, Himeji, Hyogo 671-2280, Japan, saitoh@eng.u-hyogo.ac.jp
[2]Tokyo University of Technology, Hachioji, Tokyo 192-0982, Japan, itoutk@stf.teu.ac.jp
[3]University of Hyogo, Himeji, Hyogo 671-2280, Japan, matsui@eng.u-hyogo.ac.jp
[4]Yamagata University, Yonezawa, Yamagata 992-8510, Japan, kamitani@yz.yamagata-u.ac.jp

The extended boundary node method (X-BNM) has been applied to a boundary-value problem of the Grad-Shafranov (G-S) equation and its performance has been numerically investigated by comparing with the dual reciprocity boundary element method (DRM). The result of computations shows that the accuracy of the X-BNM is higher than that of the DRM. Therefore, it is found that the X-BNM might be a powerful tool for solving a boundary-value problem of the G-S equation.

Index Terms—**Boundary value problems, Green's function methods, integral equations, numerical analysis, plasma simulation.**

I. Introduction

THE magnetohydrodynamic equilibrium in an axisymmetric plasma is described by the Grad-Shafranov (G-S) equation in terms of the poloidal magnetic flux. The boundary element method (BEM) has been so far applied for solving the boundary-value problems of the Grad-Shafranov (G-S) equation and has yielded excellent results [1]–[3].

On the other hand, Mukherjee *et al.* proposed the boundary node method (BNM) [4]. Since the BNM is one of meshless methods, a boundary does not need to be divided into a set of elements before executing the BNM code. In other words, input data of the BNM are simpler than that of the BEM. In addition, a smooth numerical solution is obtained because the shape function is determined by using the moving least-squares approximation. In this way, the BNM is the numerical method in which the demerit of the BEM is resolved partially.

Recently, the BNM has been reformulated without using integration cells. This method is called the extended BNM (X-BNM) [5]–[8]. The results of computations have shown that the accuracy of the X-BNM is much higher than that of the dual reciprocity BEM (DRM) [7]. In addition, it is found that the calculation speed can be improved by applying the shape functions of the radial point interpolation method (RPIM) to the X-BNM [8]. These results suggest that not only the BEM but also the X-BNM could be applied to a boundary-value problem of the G-S equation.

The purpose of the present study is to apply the X-BNM to a boundary-value problem of the G-S equation and to numerically investigate its performance by comparing with the DRM.

II. Discretization by X-BNM

For simplicity, we consider a boundary-value problem of the G-S equation in the cylindrical coordinate (r, z):

$$-\hat{L}\psi = \rho \qquad \text{in } \Omega, \tag{1}$$

$$\psi = 0 \qquad \text{on } \partial\Omega, \tag{2}$$

where Ω denotes a domain bounded by a simple closed curve $\partial\Omega$ in the r-z plane. Furthermore, ρ is a known function in Ω. In addition, $\hat{L}$ denotes the G-S operator defined by

$$\hat{L} \equiv \frac{\partial^2}{\partial z^2} + r\frac{\partial}{\partial r}\left(\frac{1}{r}\frac{\partial}{\partial r}\right).$$

By following the standard manner of the DRM, we assume that ρ is approximated as

$$\rho(r, z) = \sum_{k=1}^{M} \alpha_k f_k(r, z), \tag{3}$$

where M and α_k are the number of poles and the kth coefficient, respectively. Furthermore, $f_k(r, z)$ is defined by

$$f_k(r, z) = 2C\left(1 + \frac{r_k}{r} - 2Cd_k\right)e^{-Cd_k}.$$

Here, d_k is given by $d_k = (r - r_k)^2 + (z - z_k)^2$ and (r_k, z_k) denotes the kth pole. Moreover, C is a constant. Throughout the present study, C is fixed as $C = 10^2$.

By substituting (3) into the right-hand side of (1), (1) is transformed to the equivalent boundary-only integral equation:

$$\oint_{\partial\Omega} \frac{1}{r}\left(\psi^* \frac{\partial\psi(\boldsymbol{x}(s))}{\partial n} - \frac{\partial\psi^*}{\partial n}\left[\psi(\boldsymbol{x}(s)) - \psi(\boldsymbol{y})\right]\right) ds$$
$$= \sum_{k=1}^{M} \alpha_k \left\{ \oint_{\partial\Omega} \frac{1}{r}\left(\psi^* \frac{\partial\hat{\psi}_k(\boldsymbol{x}(s))}{\partial n} - \frac{\partial\psi^*}{\partial n}\left[\hat{\psi}_k(\boldsymbol{x}(s)) - \hat{\psi}_k(\boldsymbol{y})\right]\right) ds \right\}, \tag{4}$$

where ψ^* and $\partial\psi^*/\partial n$ denote the fundamental solution of $-\hat{L}\psi = r\delta(\boldsymbol{x}(s) - \boldsymbol{y})$ and its normal derivative, respectively. Furthermore, $\hat{\psi}_k$ and $\partial\hat{\psi}_k/\partial n$ are a particular solution of $-\hat{L}\hat{\psi}_k = f_k$ and its normal derivative, respectively. In addition, s indicates an arclength along $\partial\Omega$.

For $\boldsymbol{y} \in \Omega$, (4) can be rewritten as

$$\psi(\boldsymbol{y}) = \oint_{\partial\Omega} \frac{1}{r}\left(\psi^* \frac{\partial\psi(\boldsymbol{x}(s))}{\partial n} - \frac{\partial\psi^*}{\partial n}\psi(\boldsymbol{x}(s))\right) ds$$
$$= \sum_{k=1}^{M} \alpha_k \left\{\hat{\psi}_k(\boldsymbol{y}) - \oint_{\partial\Omega} \frac{1}{r}\left(\psi^* \frac{\partial\hat{\psi}_k(\boldsymbol{x}(s))}{\partial n} - \frac{\partial\psi^*}{\partial n}\hat{\psi}_k(\boldsymbol{x}(s))\right) ds\right\}. \tag{5}$$

As is apparent from (5), $\psi(\boldsymbol{y})$ can be calculated from ψ and $\partial\psi/\partial n$ on $\partial\Omega$. Therefore, we have only to obtain the solution and its normal derivative on the boundary.

For the purpose of obtaining ψ and $\partial\psi/\partial n$ on $\partial\Omega$, let us discretize (4) and (2). If N nodes are placed on $\partial\Omega$, RPIM shape functions ϕ_i's [8] can be easily determined. Furthermore, ψ and $\partial\psi/\partial n$ are assumed as

$$\psi(\boldsymbol{x}(s)) = \sum_{i=1}^{N} \phi_i(s)\,\psi_i, \qquad \frac{\partial\psi(\boldsymbol{x}(s))}{\partial n} = \sum_{i=1}^{N} \phi_i(s)\,q_i,$$

where ψ_i and q_i $(i = 1, 2, \cdots, N)$ are all unknowns.

Under the above assumptions, (4) and (2) can be discretized to get a linear system. By solving the linear system, we can get the distributions of ψ and $\partial\psi/\partial n$ on $\partial\Omega$. In this way, the boundary-value problem of the G-S equation reduces to the problem in which the linear system is solved.

III. Numerical Results

In this section, the performance of the X-BNM is numerically investigated by comparing with the DRM. As an example problem, we adopt the boundary value problem of the G-S equation over $\Omega \equiv (1/2, 3/2) \times (-1/2, 1/2)$ and the function ρ is determined so that the analytic solution can be given by

$$\psi = \left(\frac{1}{4} - z^2\right) \sin\left[\pi\left(r - \frac{1}{2}\right)\right].$$

In the X-BNM, the weight function used in the RPIM shape function is given by

$$w_i(s) = w\left(|s - s_i| / R_i\right),$$
$$w(r) = \begin{cases} (1-r)^3(3r+1) & ; r \le 1, \\ 0 & ; r > 1, \end{cases}$$

where s_i denotes the arclength to the ith boundary node and R_i is given in [8]. In addition, parameters used in the RPIM shape function are shown in [8].

Let us compare the accuracy of the X-BNM with that of the DRM. As the measure of the local accuracy, we adopt the relative error:

$$\varepsilon(\boldsymbol{x}) \equiv \frac{\left|u_{\mathrm{A}}(\boldsymbol{x}) - u_{\mathrm{N}}(\boldsymbol{x})\right|}{\underset{\boldsymbol{x}}{\mathrm{Max}}\left|u_{\mathrm{A}}(\boldsymbol{x})\right|},$$

where subscript notations, A and N, indicate analytic and numerical solutions, respectively. The error distributions for the DRM and the X-BNM are shown in Figs. 1(a) and 1(b), respectively. We see from these figures that the accuracy of the X-BNM is much higher than that of the DRM except for near corner points. From these results, it is found that the X-BNM can be applied to a boundary-value problem of the G-S equation.

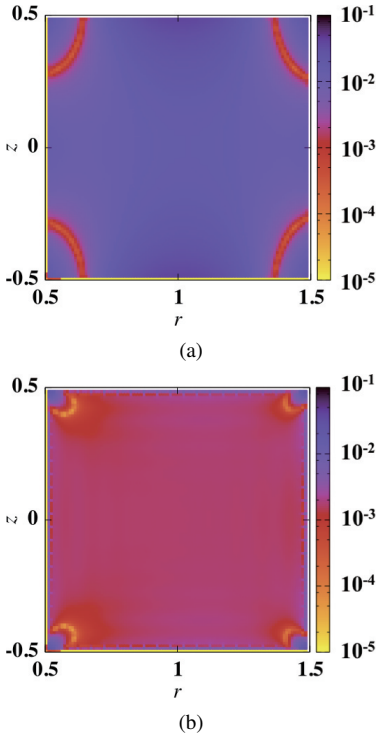

Fig. 1. Spatial distributions of the relative error $\varepsilon(\boldsymbol{x})$ $(N = 80, M = 441)$. Here, (a) the DRM with constant elements and (b) the X-BNM.

IV. Conclusion

We have applied the X-BNM to the boundary-value problem of the G-S equation and have numerically investigated its performance by comparing with the DRM. The result of computations shows that the accuracy of the X-BNM is much higher than that of the DRM. Therefore, it is found that the X-BNM might be a powerful tool for solving boundary-value problems of the G-S equation.

References

[1] M. Itagaki, J. Kamisawada, and S. Oikawa, "Boundary-only integral equation approach based on polynomial expansion of plasma current profile to solve the Grad-Shafranov equation," *Nucl. Fusion* vol. 44, iss. 3, pp. 427-437, Feb. 2004.

[2] M. Itagaki, and T. Fukunaga, "Boundary element modeling to solve the Grad-Shafranov equation as an axisymmetric problem," *Eng. Anal. Bound. Elem.,* vol. 30, no. 9, pp. 746-757, Sep. 2006.

[3] M. Itagaki, K. Nakada, H. Tanaka, and A. Wakasa, "Quasi-radial basis functions applied to boundary element solutions for the Grad-Shafranov equation," *Eng. Anal. Bound. Elem.,* vol. 33, no. 11, pp. 1258-1272, Nov. 2009.

[4] Y.X. Mukherjee and S. Mukherjee, "The boundary node method for potential problems," *Int. J. Numer. Methods Eng.*, vol. 40, iss. 6, pp. 797-815, Mar. 1997.

[5] A. Saitoh, S. Nakata, S. Tanaka and A. Kamitani, "Development of cell-independent dual-reciprocal boundary-node method," *Information*, vol. 12, no. 5, pp. 973-984, Sep. 2009 [in Japanese].

[6] A. Saitoh, N. Matsui, T. Itoh and A. Kamitani, "Development of 2-D meshless approaches without using integration cells," *IEEE Trans. Magn.*, vol. 47, iss. 5, pp. 1222-1225, May 2011.

[7] A. Saitoh, K. Miyashita, T. Itoh, A. Kamitani, T. Isokawa, N. Kamiura and N. Matsui, "Accuracy improvement of extended boundary-node method," *IEEE Trans. Magn.*, vol. 49, iss. 5, pp. 1601-1604, May 2013.

[8] A. Saitoh, T. Itoh, N. Matsui, and A. Kamitani, "Acceleration technique for extended boundary-node method", *IEEE Trans. Magn.*, vol. 50, iss. 2, Article#: 7011404, Feb. 2014.